Performance Evaluation of Fiber-Reinforced Expansive Subgrade Soil Stabilized with Alkali Activated Binder, Lime, and Cement: A Comparative Study

Mazhar Syed[1], Anasua GuhaRay[1(✉)], and Ankit Garg[2]

[1] Civil Engineering Department, BITS-Pilani Hyderabad Campus, Secunderabad 500078, India
{p20170007,guharay}@hyderabad.bits-pilani.ac.in
[2] Civil, and Environmental Engineering Department, Shantou University, Shantou, China
ankit@stu.edu.cn

Theme: Transportation Geotechnical Engineering
Subtheme: Innovative and Sustainable Geomaterials and Geosystems

Abstract. Expansive subgrade soil exhibits a high degree of volumetric instability upon periodic moisture fluctuation, resulting in low bearing strength and loss of pavement serviceability. However, the use of conventional binders has a significant impact on the atmosphere by releasing greenhouse gases. In the present study, an attempt is made to enhance the strength characteristics of the expansive subgrade soil by stabilizing with an eco-friendly alkali activated binder (AAB) reinforced by two distinct types of fibers, polypropylene (PF) and chemically treated hemp fiber (CHF). The research also compares PF and THF reinforcement's effectiveness in AAB with the conventional lime and cement binders. AAB is synthesized by adding an aluminosilicate precursor (slag and low calcium fly ash) to the alkali activator solution for sodium hydroxide and sodium silicates. In the alkaline binder, a minimum water to solids ratio (w/s) of 0.4 is maintained. The effects of varying PF and CHF content in lime, cement, and slag-fly ash-based AAB soil mixture is evaluated through a series of tests, including swelling potential, compressive shear, strength, and penetration resistance tests. California bearing ratio (CBR) is chosen as a subgrade performance indicator for both PF and CHF reinforced soil. Reliability analysis using Monte Carlo Simulation (MCS) is further conducted to determine indices for CBR and strength tests that help to analyze the impact of uncertainties associated with the design of the fiber-reinforced AAB treated subgrade layer. Microstructural and morphological studies are carried out for lime, cemented, and AAB treated soil reinforced with PF and CHF. It is observed that PF reinforced soil has achieved a higher interfacial bonding with strong interlocking density under low tensile and shrinkage cracking compared to other fibers. The study also shows that the subgrade strength improvement under higher fiber dosages is prominent when AAB is used as an additive compared to lime and

W. J. Steyn et al. (Eds.): GeoChina 2021, SUCI, pp. 118–139, 2021.
https://doi.org/10.1007/978-3-030-79857-4_8

cement. The reliability analysis results show that the optimum dosages of fiber and slag-fly ash ratio in AAB-soil mixture are essential factors for strengthening the subgrade parameters.

Keywords: Expansive subgrade soil · Alkali activated binder · Polypropylene fiber · Hemp fiber · Reliability analysis

1 Introduction

Expansive subgrade soils undergo large volumetric changes (heave/shrink) due to moisture imbalance and exhibit cracking upon desiccation, alters the long-term sealing effect. This periodic volumetric stability fluctuation is majorly attributed to the existence of montmorillonite and smectite group. The annual cost of repairing and restoring damaged structure due to expansive soil instability is projected at $9 billion in the US, $1 billion in China, and $0.5 billion in the UK. Between 1970 and 2000, the total annual loss increased by around 140%, with just $4 billion for paving and lightweight structures (Saride and Dutta 2016). The use of conventional cemented binders effectively reinforced the subgrade bearing ratio and regulated the swelling potential. However, the production of these binders contributes to 7–8% annual greenhouse gases, and by 2050 the growth in binders demand will reach up to 200% worldwide (Bell 1996). A new approach to efficiently reinforce the weak soil is the combined use of industrial by-products (such as cement kiln dust, fly ash, ashes, blast furnace slag, and bagasse ash) with low-carbon binders as a complete or partial replacement of portland cement or lime binder (Amadi 2014; Miao et al. 2017; Yong and Ouhadi 2007).

Usage of low carbon binders like Alkali Activated Binder (AAB) is another useful approach for improving the weak subgrades soil. AAB is a polymeric long-chain compound of aluminosilicate sodium matrix synthesized from pozzolanic precursors (Davidovits 1994). Envirosafe AAB offers two benefits as it limits the conventional binder's demand and saves the landfill related costs of dumping fly ash-slag. It also has superior workability, higher mechanical performance, and excellent durability with a low carbon footprint (80% less CO2) than cement binder (Provis and van Deventer 2014; Syed et al. 2020a: 2020b). Rios et al. (2016) compared the soil structural performances treated with alkali activated and cement binder. They observed that the alkaline soil specimen attained higher mechanical resistance with long-lasting strength. Miao et al. (2017) proposed an optimal alkaline mixture of 10% volcanic ash with 7% KOH on geopolymerised expansive soil, where UCS increased by 62% and swelling reduced by 43%. Jiang et al. (2018) highlighted that the subgrade strength parameters and durability of lightweight alkali activated slag mixed clayey soil sand was higher than the lightweight Portland cement binder.

Although the compressive resistance of alkaline soil improved effectively, it contributed to weak tensile and flexural strength. Shrinkage cracking is a crucial issue in the summer season, as it is expected that this form of soil will shrink (Pourakbar et al. 2016; Tang et al. 2016). The issue of soil tensile cracking can be overcome by reinforcing the discrete fibers. The random inclusion of fiber reinforcement does not prevent the propagation of soil crack but indirectly regulates the number and width of shrinkage

cracking behavior (Moghal et al. 2018b). In recent years, many researchers have proved the effectiveness of fibers reinforcement with cementitious materials in different soils and considered the excellent earth reinforcement material for soil strengthening (Sudhakaran et al. 2018; Tang et al. 2016; Wei et al. 2018). Moghal et al. (2018a) compared the CBR behavior of 6% lime blended polypropylene fiber cast and fiber mesh as soil reinforcement and concluded that the lime-fiber CBR is a good performance subgrade strength indicator. While the geopolymerization process is recently used in geoengineering applications, there is still limited study on the combination of fiber reinforcement with fly ash-slag dependent AAB in expansive soil.

In this study, an attempt has been made to strengthen the subgrade strength parameters of slag-fly ash AAB-soil reinforced with different fibers. This research's primary focus is to evaluate the geotechnical behavior of AAB treated expansive soil reinforced with randomly mixed polypropylene (PF) and chemically treated hemp (CHF) at various slag/fly ash ratios in the alkaline solution. The study also aims to compare the effectiveness of geomechanical characteristics among AAB, lime, and cement-treated fiber-reinforced soil. An effort has been made to improve the durability of the fiber and soil-fiber interaction by chemically processing the hemp fiber with 10 M of NaOH. A series of microstructural analyses were also carried out to examine the mineralogical and molecular bonding behavior. Moreover, the uncertainties in AAB-fiber-soil mixtures' subgrade strength behavior are predicted through reliability analysis for failure against the California bearing ratio (CBR) strength test by Monte Carlo Simulation (MCS) method.

2 Materials Used

2.1 Raw Materials

The expansive soil from the Nalgonda region of Telangana was obtained in the present analysis. Disturbed samples were obtained from 30 cm below the soil surfaces. The in-situ moisture content, as determined in the field, was approximately 1.46%. In the laboratory, this soil was pulverized and then oven-dried before use. The soil was listed as Highly Compressible clay (CH) as per the Unified Soil Classification System (USCS). Class F fly ash and slag from the Ramagundam thermal power plant and JSW cement India limited, Andhra Pradesh, were collected, respectively. Ordinary Portland cement (53 grades) and hydrated lime were procured from Finechem, Hyderabad. Table 1 presented the basic physical-mechanical properties of soil, polypropylene, and hemp fibers, as calculated in the ASTM test method. The grading curves of particle sizes of fly ash, slag, untreated, and AAB treated soil were shown in Fig. 1.

The elemental compositions of expansive soil, fly ash, slag, polypropylene, untreated, and chemically treated hemp fiber were summarized in Table 2. Slag and Class F fly ash (low calcium as per ASTM C618-17a) was procured from JSW Cement Ltd., Andhra Pradesh, and National thermal power corporation (NTPC) Ramagundam, respectively. The chemical compound present in raw materials was obtained from X-ray fluorescence (XRF) analysis using the PANalytical Epsilon-1 spectrometer. When interacting with high-energy X-radiations under 7kV excitation voltage, atoms' activity was examined by the significant elements in soil, fibers, and other raw materials by maintaining constant

Table 1. Soil and fiber material properties

Properties	Soil	Properties	PF	HF
pH	8.2	Density (kg/m^3)	910	820
Specific gravity	2.58	Diameter (mm)	0.033	0.035
Sp. Surface area (m^2/g)	49	Tensile strength (MPa)	330	110
Free swell index (%)	89	Elastic modulus (MPa)	3500	3400
Liquid limit (%)	63	Burning Point (^{0}C)	588	–
Plasticity index (%)	38	Hemicellulose (%)	–	11
Dry density (g/cc)	1.6	Cellulose (%)	–	65
Moisture content (%)	24	Lignin (%)	–	6
Tensile strength (kPa)	6.6			
Compression strength (kPa)	186			
Soaked CBR (%)	1.93			

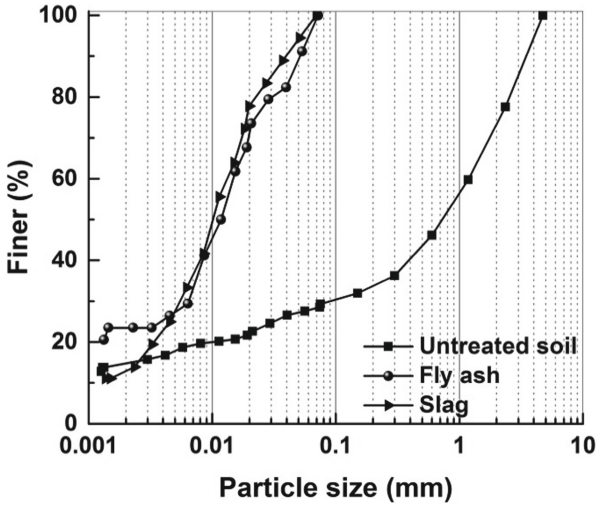

Fig. 1. Particles size distribution curves of fly ash, soil, and slag

temperature and air pressure. The main components of fly ash comprise 47.1% silicon dioxide (SiO2), 20.1% aluminum oxide (Al_2O_3), 15.3% magnesium oxide (MgO), and 7.1% ferric oxide (Fe_2O_3). In addition, slag was rich in calcium oxide (CaO) of around 40.6%, with (>52%) of AL_2O_3, MgO, and SiO_2 content. The presence of high calcium content in the slag can result in Calcium Silicate Hydrate (C-S-H) formation, which coexisted in the alkaline soil mixture with pozzolanic products. The leaching of heavy metals from the fly ash and slag combination was very negligible. The fly ash and slag composition of heavy metals such as chromium (Cr), arsenic trioxide (AS_2O_3), lead

oxide (PbO), and zinc oxide (ZnO) were not found. Chemical compounds in fly ash and slag (such as Cao, MgO) can also easily monitor pH and soil leachate.

India produces almost 95–110 million tons of fly ash and slag from power and steel plants every year(IRC-SP-20–2002). In developing countries like India, the disposal of industrial waste by-products (such as slag and fly ash) is a big concern. The utilization of these wastes by combining with cementitious material in the soil enhances the subgrade properties, thereby preventing the need for disposal. These techniques save the associated costs of dumping into landfills and eliminate the demand for traditional binders. As most of these plants donate fly ash and slags, the cost of producing AAB is also lesser than that of Portland cement. AAB is found to act as an auxiliary cementing binder with a higher grade of serviceability performances with low ecological harm. India is the second-largest producer of fiber in the world. These fibers (synthetic and chemically treated natural fibers) are not affected by salts in soils, have low biological and ultraviolet degradation and survive in high-temperature conditions. Practically, the fiber-AAB-soil mixtures have been thoroughly mixed using a rotavator and layer compacted using a roller compactor. Practically, the fiber-AAB-soil mixtures have been thoroughly mixed using a rotavator and layer compacted using a roller compactor. Most of the construction of subgrade layers under Pradhan Mantri Gram Sadak Yojna (PMJSY) of unpaved roads (low-volume roads) and rural roads are stabilized with chemical binders using rotavator and compactor. Combining fly ash, slag, and fibers in the alkaline soil can offer a sustainable and economical solution for improving the poor subgrade properties.

Table 2. Chemical composition of raw materials

Elements (%)	Expansive soil	Fly ash	Slag	PF	HF	CHF
Magnesium Oxide	17.93	15.30	18.38	90.3	0.02	0.2
Aluminum oxide	12.46	20.17	12.09	0.00	2.90	2.9
Silicon dioxide	43.49	47.13	22.66	00.0	3.70	4.11
Phosphorus oxide	01.27	01.24	00.00	1.30	14.1	13.2
Sulfur trioxide	00.43	00.57	01.74	1.40	0.20	10.2
Chlorine	00.78	03.65	00.55	2.3	24.7	28.9
Potassium oxide	03.76	02.55	00.60	0.6	8.71	5.1
Calcium oxide	08.97	03.11	40.65	2.4	33.4	25.3
Titanium dioxide	01.34	02.00	01.23	0.1	1.5	0.95
Ferric oxide	09.34	07.12	01.11	0.8	10.6	7.4

2.2 Fiber Reinforcement

Two types of fibers, polypropylene and hemp fiber, used as reinforcement material in this study, were obtained from Go-green industries, Tamil Nadu. Based on soil-fiber contact, interlocking density (greater contact area with higher gripping around the fiber and pozzolanic compounds), interfacial bonding, and friction, a constant length of 12 mm and

25 mm were chosen for polypropylene and hemp fiber (Bordoloi et al. 2017; Moghal et al. 2017). Hemp fiber was chemically treated with 10M sodium hydroxide (NaOH) for 28 days to improve its quality and service life in the soil before being used as a soil reinforcement (Sudhakaran et al. 2018). The primary reasons for using polypropylene and hemp fiber in the AAB-soil are their negligible effects on the environment, sustainability, local accessibility, cost-effectiveness, and the ability to monitor the soil dispersivity, swell-shrink potential in the expansive soil (Syed and Guharay 2020; Mazhoud et al. 2017; Tang et al. 2007). Several studies have shown the research on the effectiveness of fiber reinforcement (type, length, and amount) with conventional cementitious binders on untreated soil. However, in past findings, the microstructural and geomechanical activity between polypropylene chemically modified hemp fibers in expansive soil has not been compared. This paper contributes to this where the influence of the effect of two fibers (PF and CHF) on AAB mixed soil was studied and compared with different cementitious binders. Figure 2 displayed polypropylene's surface images, untreated, and chemically treated hemp fibers using a stereomicroscope. Alkali activated binder (AAB) was generated by mixing alkaline solution consisting of sodium hydroxide and sodium silicate (mass ratio 10.57:29.43) in precursors of aluminosilicate (such as slag and fly ash class F). Within the alkaline binder, the fly ash and slag ratios are varied to get the optimal blend.

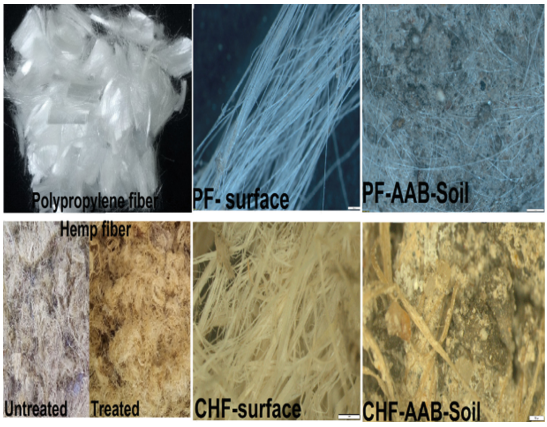

Fig. 2. Stereomicroscopic images of PF and CHF reinforced AAB soil

2.3 Sample Preparation

The expansive soil was mixed separately with 5% dry cement, 5% lime, and 5% AAB paste (by dry mass of soil) at different slag/fly ash ratios (0/100, 20/80 40/60 proportions) in the AAB. 5% binder content in the soil was selected as optimum based on pH, alkaline reactivity, binding efficiency with low greenhouse gas emissions, and cost-effective compared to other dosages (Yong and Ouhadi 2007). Binder mixed soils were manually compacted in separate containers into three layers with a steel compactor rammer.

Moreover, compacted soil samples were covered with a moist jute bag for 28 days at room temperature for continuous curing. Before random mixing of polypropylene and chemically treated hemp fiber (0.2, 0.4, 0.6, and 0.8% dry weight of soil) in AAB, Lime, and cemented soil mixtures, the soil was oven-dried at 110 °C for 24 h. The terminology used for fiber-reinforced AAB, lime, and cemented soils was defined in Table 3.

Table 3. Sample definition of mixture proportion of fiber-reinforced soils

Sample designation	Sample definition
E.A5(Sm/Fn).Px E.A5(Sm/Fn).Hy m + n = 100 E.C5 E.L5 E.A_5 (S_0/ F_{100})$P_{0.8}$ E.A_5 (S_{20}/ F_{80})$P_{0.8}$ E.A_5 (S_{40}/ F_{60})$P_{0.8}$ E.A_5 (S_0/ F_{100})$H_{0.8}$ E.A_5 (S_{20}/ F_{80})$H_{0.8}$ Similarly for other samples	E = Expansive soil; A_5 = Mixing of 5%Alkali Activated Binder in the soil; C_5 = Mixing of 5% Cement in the soil; L_5 = Mixing of 5% Lime in the soil; S = slag; F = Fly ash; S_m /F_n = slag-fly ash ratio in the AAB mixture (0/100, 20/80 and 40/60); P = Polypropylene fiber; H = Chemically treated hemp fiber; m = Slag content in the AAB mixture (0, 10, 20, 30, and 40); n = Percentages of fly ash in the AAB mixture (100, 90, 80, 70, and 60); x = Percentages of polypropylene fiber mixed in soil (0%, 0.2%, 0.4%, 0.6% and 0.8%); y = Percentages of chemically treated hemp fiber mixed in the soil (0%, 0.2%, 0.4%, 0.6% and 0.8%)

3 Methodology

3.1 Microstructural Characterisation

A series of microstructural experiments were conducted with Fourier-transform infrared (FTIR), X-ray powder diffraction (XRD), Surface micrographs, and Energy-dispersive X-ray spectroscopy (EDS) on untreated, lime, AAB, and cemented fiber-reinforced soils. Such studies helped to examine the changes in soil structure's mineralogy, bonding activity with fibers matrix, and their reaction products. The JASCO FTIR 4200 setup was used to perform the FTIR absorbance spectroscopy through K.Br. Pellet arrangement. The spectral absorbance range for both untreated and chemically treated soils was 4000–500 cm^{-1} was selected. XRD was carried out using the RIGAKU Ultima-IV diffractometer with an operating step of 0.02° for 2θ values. At 40 mA and 40 kV, CuKα rays were passed from 0° to 80° of 2θ at 2 s per step. Using Thermo Science Apreo SEM given by FEI at various spot regions and magnifications, soil surfaces and elemental composition were analyzed. The EDS spectra are calculated using Aztec's Oxford Instruments analyzer method. For a mass sample of 20 mg up to 800 °C under a nitrogen-rich atmosphere, TGA on both untreated and chemically treated hemp fiber was analyzed using Shimadzu/DTG-60 with a 10 °C/min heating rate.

Before and after applying cementitious binders in the soil, these tests help examine mineralogy and molecular bonding behavior variation. Moreover, it also ascertains the alterations in soil structure morphology, with fibers matrix, and their reaction products. FTIR and XRD provide qualitative information about the chemical composition of

the materials. Stereomicroscopy also offers qualitative information about the materials' physical characteristics. SEM, in conjunction with EDS analysis, is carried out in order to gain quantitative information.

3.2 Geotechnical Characterisation

A series of undrained shear (according to ASTM D2166–00), consolidation (following ASTM D2435–04), California bearing ratio (ASTM D1883–16), and flexural strength (ASTM D-1635) tests were performed for lime, cement, and AAB treated soil and reinforced with different fiber dosages. Both proportions of soil samples treated with slag/fly ash-based ratios of AAB mixture, cement, and lime were prepared at the respective MDD and OMC values.

The soil swell-consolidation tests were performed using the 2 cm height and 6 cm diameter one-dimensional Oedometer following the ASTM D2435–04 standard. Swell potential and e-log (p) curves were determined against a seating pressure of 6.25 kPa with different cementitious binder mixed soil specimens by ensuring their dry density. Swell potential (S%) was recorded as the soil thickness (H) increase ratio to the specimen's original thickness (H). In standard UCS split molds, both fibers reinforced soils were compacted in a mold of diameter 3.8 cm and height 7.6 cm. An automatic, strain-controlled compression system with a maximum 20 KN capacity at a fixed strain rate of 0.125 cm/min was used for the UCS test. Soaked CBR tests on lime, cement, and AAB with varying fly ash-slag composition were conducted as per ASTM D-2435. Specific soil specimen binders and fiber dosages were compacted at their MDD-OMC values in a standard CBR mold of 15 cm diameter and 17.5 cm height. Compacted soil-fibers specimens were soaked in water for four days with a 5 kg surcharge before testing at a fixed strain rate of 0.125c m/min through a 50 mm diameter plunger.

In the Marshall Stability Machine, soil-fiber tensile tests are carried out by adding a loading strip of 12.5 mm to the load frame by preparing the 100 mm cylindrical sample of height 80 mm with a steady strain rate of 50.5 mm/minute during the tests. Similarly, the flexural strength was carried out by molding a 280 mm long flexure beam, 70 mm wide, and 70 mm thick in a three-point bending flexure machine. The flexure beam was compacted into five layers using a 3 kg steel rammer with a free fall of 310 mm. The beam specimens were removed after 48 h and mounted on two supports having a span length of 130 mm under a fixed loading strain rate of 0.1 mm/min. The following equation gives the ITS (S_t), modulus of rupture (R_m), and elastic modulus in mPa.

$$S_t = \frac{2\,P_{max}}{\Pi td} \tag{1}$$

P_{max} = maximum load at which failure of soil sample occurred (N),
t = thickness of soil specimen (mm), d = diameter of the soil specimen (mm).

$$R_m = \frac{3p_{ult} * l}{2bh^2} \tag{2}$$

$$E = \frac{p_{ult} * l^3}{4\Delta bh^3} \tag{3}$$

P_{ult} = ultimate breaking load at which sample failure occurred in (N),
l = length of beam specimen (mm), b = width of the beam specimen (mm),
h = depth of the beam specimen (mm), Δ = deflection of beam (mm).

3.3 Reliability Analysis

The stability of structures is always impaired if they do not incorporate geotechnical variables' randomness into their design. The principle of reliability analysis is a proven mathematical method that considers these uncertainties of field variables (GuhaRay and Baidya 2015). The nonlinear form of equation used for regression analysis for both fibers reinforced AAB-soil is as follow below:

$$y = p\,(D_{Fiber}) + q(D_{SFR}) + r\,(D_{Fiber})^2 + s(D_{Fiber} * D_{SFR}) + t(D_{SFR})^2 + K_0 \quad (4)$$

Where p, q, r, s, and t = regression coefficient; K_0 = constant; D_{SFR} = dosage of slag/fly ash ratio in the alkaline solution; D_{Fiber} = dosage of polypropylene and chemically treated hemp fiber in AAB-soil respectively.

$$CBR_{PF} = 6.7198 \times (D_{PF}) + 8.9886 \times (D_{SFR}) - 1.4179 \times (D_{PF})^2 + 6.1394 \times (D_{PF} \times D_{SFR}) - 7.4595 \times (D_{SFR})^2 + 4.7295 \quad with\ R^2 = 0.993 \quad (5)$$

$$CBR_{CHF} = 3.7237 \times (D_{PF}) + 8.8624 \times (D_{SFR}) + 1.8611 \times (D_{PF})^2 + 3.9371 \times (D_{PF} \times D_{SFR}) - 7.2152 \times (D_{SFR})^2 + 4.7545\ with\ R^2 = 0.996 \quad (6)$$

Table 4. Statistics of input random variables

Random variables	Statistics		
	Mean (μ)	COV (%)	Distribution
D_{PF} & D_{CHF}	0.2, 0.4, 0.6, & 0.8%	5%	Normal
DSFR	0.0, 0.25, & 0.66	5%	Normal
CBR_{min}	7 (%)	10–40%	Log-normal

For predicting the uncertainties in alkaline subgrade fiber-reinforced soil performance, a minimum specified soaked CBR (CBR_{min}) value is assigned from experimental observations. Table 4 describes the independent random variables, such as fiber dosages (D_{PF} & D_{CHF}) and the slag-fly ash ratio (D_{SFR}), defined by their mean and coefficient variation coefficient. The coefficient of variation (COV) of D_{PF}, $D_{CHF,}$ and D_{SFR} was considered as 5% based on variations in loading conditions and testing environment. The COV for CBR_{min} was considered in the range of values proposed in the literature as 10–40% (Moghal et al. 2017). The present analysis presumed that the soaked CBR_{min} for both fiber-AAB-soils was approximately equal to 7% against the subgrade failure.

Monte Carlo simulation (MCS) was used to calculate the probability of failure (P_f) for different fiber content and slag-fly ash ratio in the AAB subgrade soil by simulating 30,000 variables in commercially available MATLAB software. It was consistent with Zevgolis and Bourdeau (2010) that the value converged for approximately 30,000 realizations. The P_f for CBR was defined as follows:

$$P_f = P(CBR - CBR_{min} < 0) = P(\frac{CBR}{CBR_{min}} < 1) \tag{7}$$

The reliability index (β) is defined as follows.

$$\beta = log\ inv\ (P_f) \tag{8}$$

4 Results and Analysis

4.1 Microstructural Studies

4.1.1 Fourier Transfer Infrared Spectroscopy (FTIR)

In order to support the new functional group of soil crystallinity, the untreated, AAB, and cement treated soils were analyzed through FTIR spectroscopy. The relative transmittance spectra curve of untreated soil, shown in Fig. 3, was generally characterized by montmorillonite at 3660 cm^{-1}, followed by 3460 cm^{-1} for O-H stretching bound groups and water. A slight reduction of montmorillonite peak intensity was observed in cemented soil at around 3650 cm^{-1}. This decrement might be due to chemical weathering action on clay surfaces (Miao et al. 2017). Furthermore, the broadband was observed at 1650 cm^{-1} and 1440 cm^{-1} corresponded to C = C alkene and C-O-H's stretching vibration in both untreated soil and AAB-cemented soil. Due to the active presence of Na in the soil matrix, this carbonation reaction can be inducted. The band attributed a range of 1004–1029 cm^{-1} to the asymmetric stretching vibration of the Si-O and Al-O group. Some quartz was also present at 798 cm^{-1} with a lower frequency of Si(Al)-O stretching vibrations. The Si-Al in-plane bending vibration was located in the wavenumber of approximately 560 cm^{-1}. Related bonds with a chemical change of around 20 cm^{-1} from untreated soil, AAB, and cement treated soil were seen in the spectrum peaks.

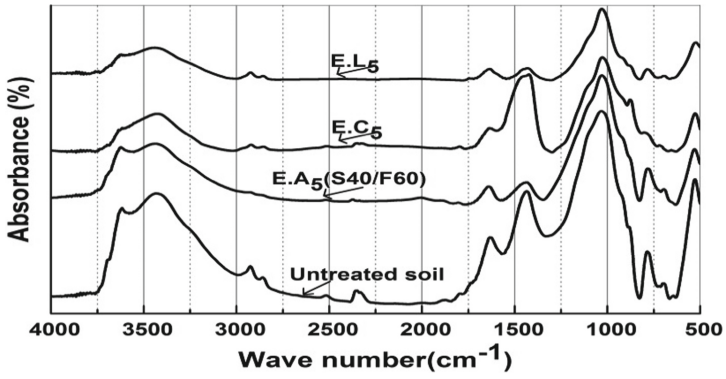

Fig. 3. FRIR spectroscopy of untreated soil, AAB, cement, and lime treated soil

4.1.2 X-ray Diffraction (XRD)

XRD is a fundamental investigative technique providing a broad range of comprehensible data on crystalline compounds found in clay minerals. Figure 4 showed the powdered XRD profile for untreated soil, AAB, cement, and lime treated soil. Untreated soil exhibited the crystalline peaks of quartz (Q), calcite (C), muscovite (Ms), and montmorillonite (M) (Sivapullaiah et al. 2010). The diffraction pattern of montmorillonite (M) and muscovite (Ms) decreased for AAB and cemented soil. XRD showed additional mullite (Mu) peak in AAB treated soil, indicating the active dissolution of sodium aluminosilicate compounds in soil by geopolymerisation (Miao et al. 2018). In addition, the cementitious compounds such as calcium silicate hydrate (CSH) and calcium aluminum hydrate (CAH) along with kaolinite (K) occurred in lime and cemented soil (Al-Mukhtar et al. 2012). The formation of these minerals might be because of the rapid hydration and pozzolanic reactions in the soil. For both untreated and cementitious binder treated soils, flatter portions of XRD indicated the amorphous phases.

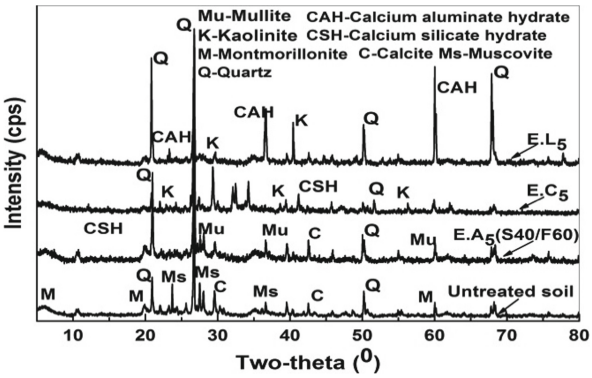

Fig. 4. XRD crystalline peaks of untreated soil, AAB, cement, and lime treated soil

4.1.3 Scanning Electron Microscope (SEM)/EDS Analysis

The surface micrographs of untreated soil, lime, cement, and fiber-reinforced AAB treated soils at different magnifications were presented in Fig. 5 (a-g). The untreated soil exhibited dispersed undulating microstructure in Fig. 5a, which was typically found in the clay matrix's montmorillonite-smectite group and imparted high volumetric instability and low shear strength upon moisture variations (Sivapullaiah et al. 2010). The soil–lime mixtures at 28 days (Fig. 5b) showed a series of floppy-like aggregated crystalline microstructure exhibited due to rapid exothermic cation exchange around the clay particles. In Fig. 5c, the cemented soil morphology developed into bladed crystals (needle shape) with long slender prism texture (Al-Mukhtar et al. 2012). Besides, the soil matrix showed the filling of voids with rods like ettringite needles along with cementitious compounds and aggregated particles. AAB soil based on fly ash-slag changed the clay composition by shaping the flocculated structure with a combination of hollow spherical particles (unreacted fly ash) and thin, smooth pitted gel layers (reacted fly ash)

in Fig. 5d. Figures 5e and f demonstrated the discrete reinforcement of polypropylene and hemp fibers in AAB soil as a spatial thread groove network. Hence, the fiber inclusions restricted the relative changes in crack widths' movement by actively retaining the clay particles through their interfacial friction. A detailed elemental composition of the quantitative graph is provided in Fig. 5g in order to support the above micrographs.

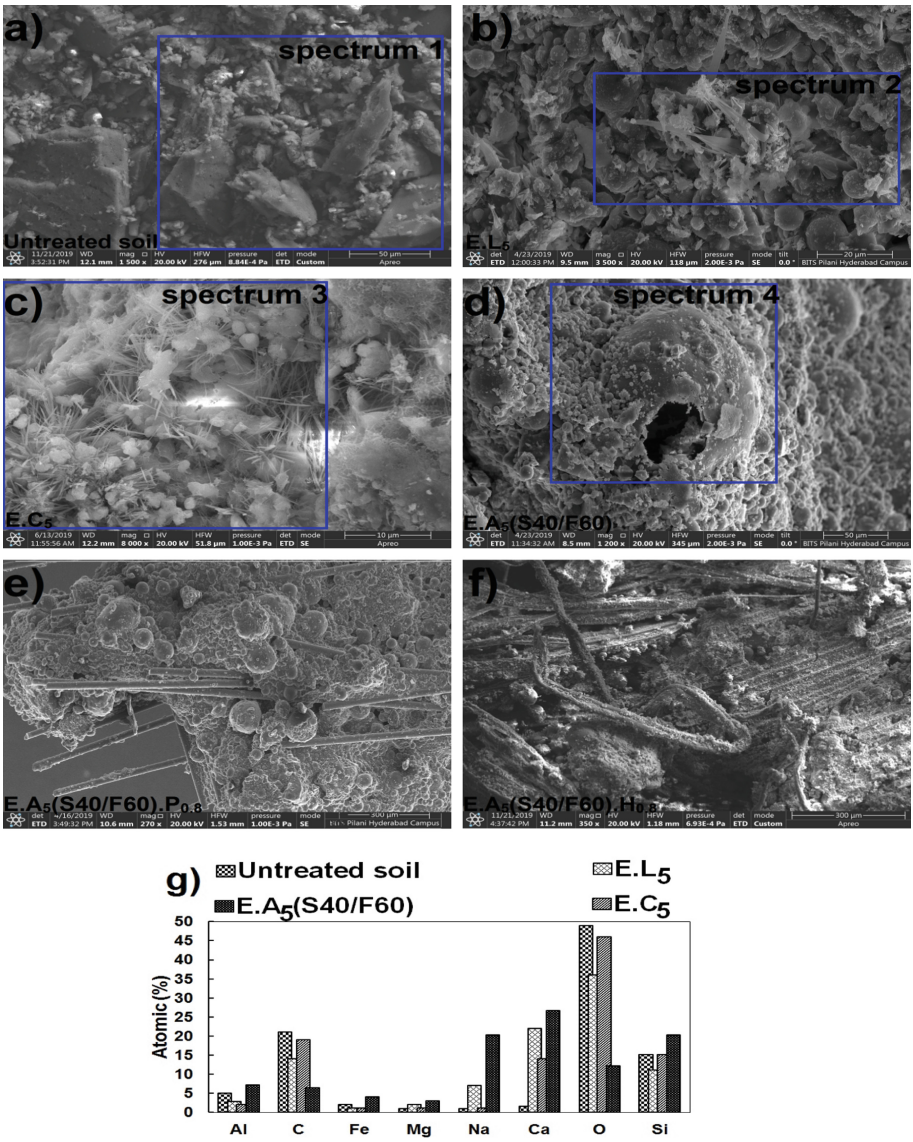

Fig. 5. SEM/EDS images of a) Untreated soil b) Lime-soil, c) Cemented-soil, d) AAB-soil, e) PF-AAB soil, f) CHF-AAB soil, g) Elemental compositions of soils.

4.1.4 Thermogravimetric Analysis (TGA)

Figure 6 shows the TGA curve for hemp fibers before and after chemical treatment in the form of mass loss upon temperature. The first significant loss happens in both fiber samples at around 110 °C and 300 °C. This reduction is due to the removal of free moisture and evaporation of volatile matters. The second mass loss is associated with biomass ranged at 350–390 °C, and this can happen due to the decomposition of hemicellulose and cellulose (Syed et al. 2020a). Comparing the results with parent fibers, the bands' position for treating fibers has changed and shifted towards the right side. The changes in the positions of peaks in treated fibers confirm the alteration of fiber surface structure and the formation of new chemical compounds after NaOH's addition. Further, it is also pointed out that the percentage of initial mass loss for coir fiber (6–8%) is relatively higher than hemp (4–5%). The low mass loss in treated fiber maybe because of encapsulation with NaOH around the fiber surfaces. TGA curves beyond 600 °C show minimal losses and mostly follow asymptotic behavior.

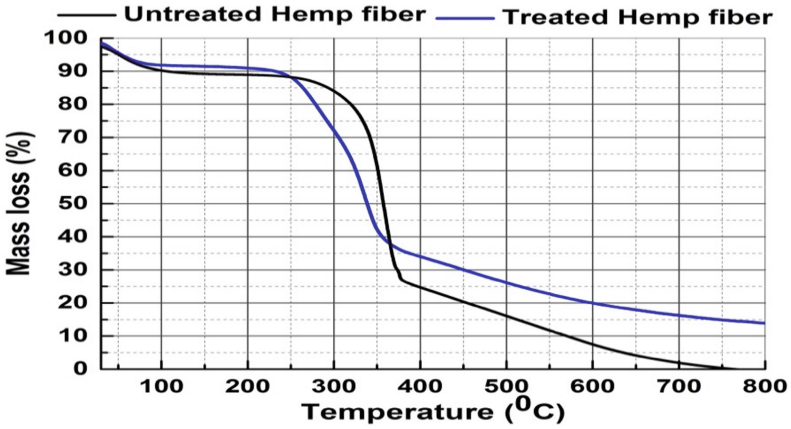

Fig. 6. TGA curve of untreated and chemically treated hemp fiber

4.2 Geotechnical Characterisation

A set of geomechanical tests on cemented, lime, and AAB treated soil were conducted at different slag/fly ash ratios as per ASTM norms. For comparison, the basic geoengineering properties are summarized in Table 5.

4.2.1 Consolidation

Figure 7(a-b) exhibited typical consolidation and swelling potential curves of soil amended with lime, cement, and AAB mixture at varying slag-fly ash ratios. Figures 7a and b revealed that the untreated soil attained the highest swelling potential and equilibrium void ratio with steeper slope relative to chemical binder reinforced soils. The volumetric expansion activity of lime and AAB stabilized soils was reduced marginally.

Table 5. Basic geotechnical tests for lime, cement, and AAB treated soils

Properties	E.L5	E.C_5	E.A_5(S0/F100)	E.A_5(S20/F80)	E.A_5(S40/F60)	Test method
MDD (kN/m^2)	16.98	17.82	17.65	18.01	18.20	ASTM-D654
OMC (%)	20.18	18.66	19.21	18.46	18.32	ASTM-D654
PI (%)	24.11	21.26	22.69	20.75	19.9	ASTM-D4318
K (m/sec) (10^{-9})	0.896	0.846	0.82	0.864	0.0840	ASTM-D5084
Ls (%)	6.56	6.24	6.39	6.22	6.08	AS1289-C177
CC	0.16	0.14	0.16	0.15	0.14	ASTM-D2435
FSI (%)	41.26	36.42	38.16	33.8	31.9	IS 2720–40

When replacing fly ash with slag content in the AAB soil increased, the void ratio and swelling percentages further decreased. Minimizing the soil compressibility behavior upon addition of lime and the pozzolanic precursor is aided to activate the cationic exchange process, resulting in the formation of more soil flocculated matrix. The surface area and moisture retention potential of soil samples decreased due to the transition to a flocculated structure. Furthermore, in the existence of alkali solution, the rupture of sodium aluminosilicate precursors with a subsequent combination of cations might arise under geopolymerization, which capsulated the clay particle surfaces, resulting in less moisture absorbance and heaving (Miao et al. 2017; Rios et al. 2016). Besides, cemented soil effectively reduced the void ratio from 1.06 to 0.84 and the swell potential from 13.6 to 6.4%, respectively. In the presence of soil moisture, cemented soil actively generated the calcium-based alumina-silicate hydrated gel from its available calcium and silica, which indirectly influenced to limit the soil volume changes. Thus the consistent formation of new mineralogy in cementitious binder regulated the soil compressibility activity efficiently.

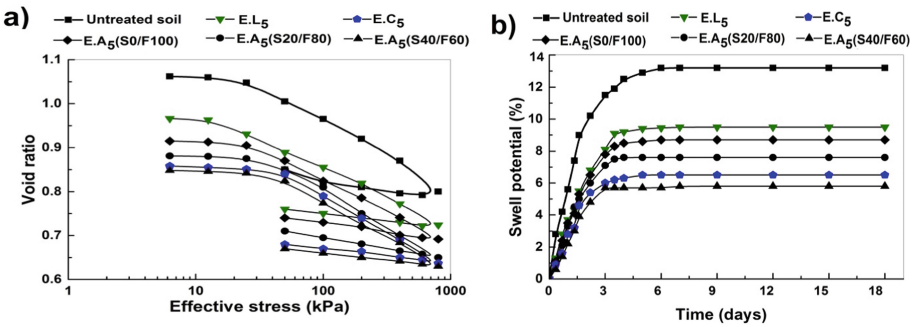

Fig. 7. Consolidation curve of lime, cement, and AAB treated soils a) void ratio versus effective stress b) Variation of swelling potential

4.2.2 Unconfined Compression Strength (UCS)

Figure 8 showed the variation of UCS values treated with three different chemical binders (lime, cement, and AAB) reinforced with polypropylene (represented in solid lines) and hemp fiber (dotted lines) at various percentages. It was evident from the results that the combined addition of cemented binders with fiber reinforcement shows a significant improvement in the shear resistance capacity. The UCS trend of mixed lime, cement, and AAB soils increased with increasing fiber dosages. The shear strength increment was more consistent with the alkaline binder through a higher ratio of slag-fly ash in both fibers reinforcement. Combining fly ash with slag volume in the AAB soil matrix was advantageous as it increased the level of geopolymerisation process and altered the mineral composition by formulating the active cementitious compounds across the fiber clay surfaces (Miao et al. 2017; Pourakbar et al. 2016; Zhang et al. 2013). On the other hand, the percentage gain in compressive shear strength was increased by around 32% for lime-fiber and 44% fiber-cemented soil mixtures. The substantial variations might be due to hydrated cementitious silicate gel formation in cemented soil upon the activation of hydration reaction. Moreover, the improvement was much greater in PF-soil than CHF-soil reinforcement in all chemically binder mixed soils. This enhancement might be attributed to their higher interfacial friction mobilization friction and bonding produced around the fiber surfaces during loading (Moghal et al. 2017; Tang et al. 2016; Wei et al. 2018). Also, polypropylene fibers were easily distributed in the soil matrix and bear the pulling stress with a higher linkage effect than the hemp fiber. It was also noteworthy that in the AAB soil, the 40/60 slag/fly ash ratio increased 35% compressive shear resistance than 0/100 (pure fly ash). Hence the increase in fiber dosages with slag replacement (up to 40%) in the AAB soil mixtures aids in improving the compression shear resistance capacity by restricting the relative moment of fiber in the soil.

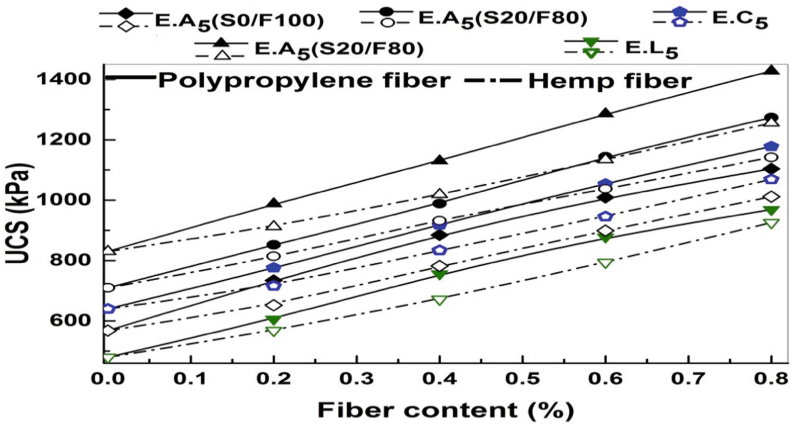

Fig. 8. UCS results of lime, cement, and AAB soil reinforced with PF and CHF at varying slag-fly ash ratio

4.2.3 California Bearing Ratio (CBR)

The effect of discrete fibers in lime, cement, and AAB treated soil mixtures on improving subgrade strength bearing ratio was calculated in terms of soaked CBR, which indirectly estimated the material's durability and its efficiencies. Figure 9 showed the soaked CBR for PF and CHF reinforced soil treated with three cementitious binders at different fiber dosages. Observations were made between the loads applied against penetration of the plunger at 2.5 mm. The CBR (both soaked and unsoaked) value of untreated soil was 1.96% and 5.5%, respectively, implying low strength bearing resistance. The efficiency of CBR penetration resistance for all chemical binders of mixed soils increased as fiber dosages increased. From the graphs, it was noticed that AAB-fiber soil specimens, dependent on slag-fly ash, had the highest CBR values than specimens of lime-admixed fiber soil. Combining fly ash with slag material in the alkaline soil mix potentially activated the cementation compounds due to the early deposition of pozzolanic substances in the presence of reactive alumina and silica soil substances (Murmu et al. 2018). Also, PF-soil had attained 8–12% higher penetration resistance in comparison to CHF-soil mixture in all cemented treated soils mixtures. The occurrence of this substantial variation in the CBR strength of PF-soil might be due to its higher interfacial confinement bonding, good surface roughness, contact area, and more significant mobilization of friction during loading (Moghal et al. 2018b; Sudhakaran et al. 2018). In addition, PF might effectively distribute specimens in the soil and offer more excellent resistance to plunger penetration. By effectively gel-forming aluminosilicate ions during soaking, the composite application of fiber and slag-fly ash in the AAB soil mix helped to form the soil-fiber spatial thread-bridge networks.

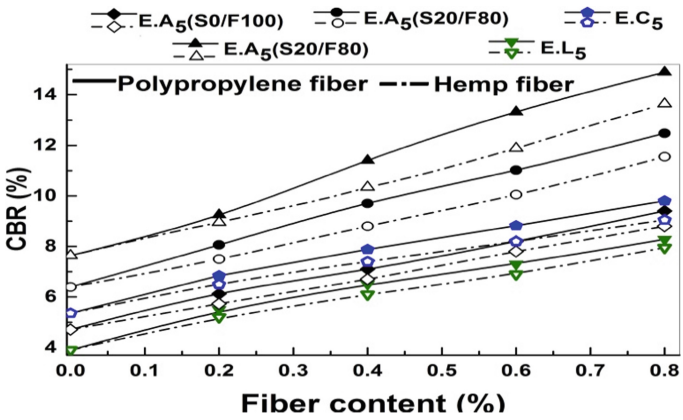

Fig. 9. Soaked CBR results of lime, cement, and AAB soil reinforced with PF and CHF at varying slag-fly ash ratio

4.2.4 Indirect Tensile Strength (ITS)

The results of ITS provide evidence to examine the effectiveness of soil fiber reinforcement by transferring shear stress to the fiber matrix that indirectly regulates soil cracking.

Figure 10 Exhibits variance of ITS values for soil treated with lime, cement, and AAB reinforced with two different fibers (polypropylene and hemp). It also reveals that the fiber type, dosage, and slag ratios play a significant role in strengthening the soil tensile property. The outcome of the ITS result follows a parallel trend with that of UCS for both fiber-reinforced treated soils. Upon comparison, slag based AAB-soil-fiber mixture attained the highest potential for tensile resistance than other cementitious binder mixed soil fiber. The marginal percentage gain in ITS performance was observed in lime and pure fly ash based alkaline soil-fiber samples. It also found that the effects of ITS on cemented and AAB soils have greatly improved between 0.2–0.6% of fiber dosages of more than 20% slag in the alkaline solution. The drastic enhancement in tensile force maybe because of bridge effect formation through interfacial friction and particles bonding around the fiber (Cristelo et al. 2015; Tang et al. 2007). Moreover, the combined addition of PF-AAB exhibits more stretching and sliding resistance over CHF-AAB-BCS soil. As a result, frictional bonding and surface roughness produce higher interlocking density and soil stiffness, indirectly overcoming the soil's brittleness (Correia et al. 2015; Elkhebu et al. 2020). Thus, the increase in fiber dosages in lime cemented and AAB soil mixtures aid to upgrade the tensile bearing efficiency by restricting the relative moment of fiber in the soil.

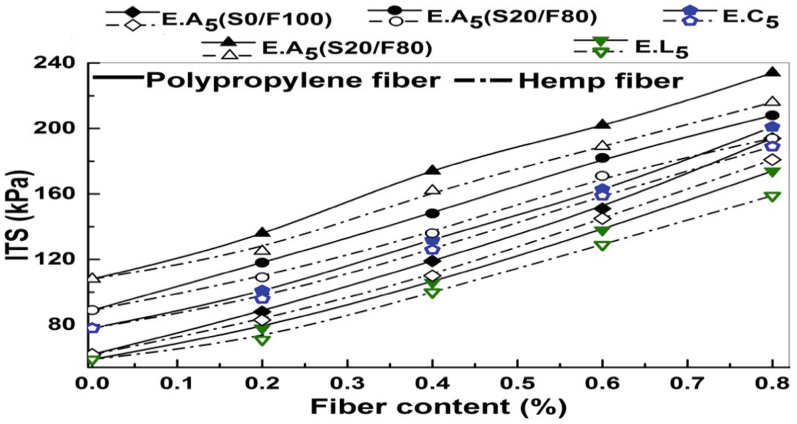

Fig. 10. Variation of ITS values for PF and CHF reinforced soil treated with lime, cement, and AAB mixtures at varying slag-fly ash ratio

4.2.5 Modulus of Rupture and Elasticity

Figure 11 (a-b) shows the flexural strength (modulus of rupture) and elastic modulus of lime, cement, and AAB treated fiber soils that are analyzed through the load-deflection curve. Figure 11a shows the results of flexural strength in the soil mixture on different combinations of cemented binders and fibers. It showed that the form of fiber and its proportions in the chemically treated soils played a leading role in strengthening flexural behavior. The flexural strength trend also follows a similar pattern, such as tensile strength on binder and fiber addition in soil. The AAB's 0.66 slag fly ash ratio was attained 16%

and 28% higher than the cement and lime fiber soil mixture. Besides, the percentage growth in flexural strength in lime and cemented soil for PF and CHF reinforced soil was marginal above 0.6% of fiber dosage. Fiber and slag dosages in the AAB-soil mixture impart the stiffness and compression shear, transforming the brittle to ductile behavior by interfacial mechanism interaction (Anggraini et al. 2016; Elkhebu et al. 2020; Pourakbar and Huat 2017). Figure 11b exhibits the variation of fiber-reinforced soil elastic modulus. In order to avoid the cluster of data, only an optimal fiber dosage (0.8%) mixed in lime, cement, and 40/60 slag fly ash ratio in AAB soils were shown for comparison. The increase in elasticity is proportional to the increase in flexural and compressive shear resistance (Figs.11a and 9). In the lime, cement AAB soil mixture, PF-soil elastic moduli are also found higher than CHF-soil. The relatively higher gain in compression shear strength in PF may be due to the higher mobilization of interfacial friction produced around the fiber (Chandra et al. 2007; Kutanaei and Choobbasti 2017; Yetimoglu et al. 2005).

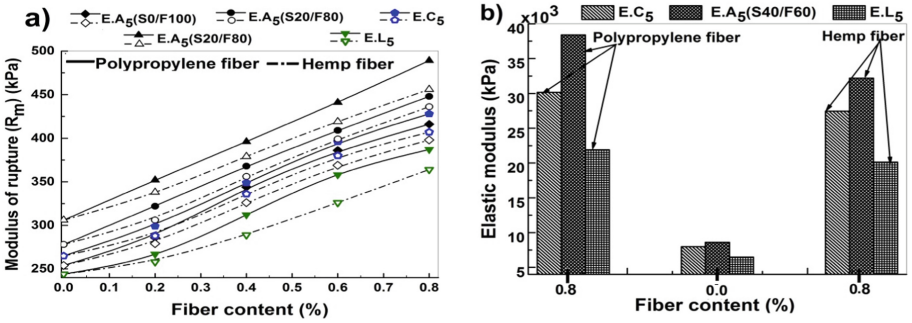

Fig. 11. Variations of a) Modulus of rupture b) Elastic modulus of PF and CHF reinforced soil treated with lime, cement, and AAB mixtures

4.3 Effect of Reliability Indices on CBR Strength

A comparison of the reliability indices for both PF and CHF AAB-soils against CBR failures is shown in Fig. 12 (a-d). In the alkaline soil mixture, the combined effect of slag-fly ash ratio and fiber reinforcement played a vital role in the magnitude of $\beta_{CBR\text{-}PF}$ and $\beta_{CBR\text{-}CHF}$ failure. For both fiber-reinforced AAB soil, the reliability results presented in these figures are obtained for a typical value of $CBR_{min} = 7\%$ at 10–40% of the variation in COV. The minimum specified CBR value ensures the safety level of reliability of subgrade strength bearing capacity at different COVs for predicting the soil-fiber behavior in terms of the stability of the subgrade material. Figure 12a and 12b indicate the CBR reliability index (β_{CBR}) maintaining CBRmin COV = 10 to 20% for different fiber dosages (0.2–0.8%). The reliability index's magnitude can be observed to increase with an increase in the slag/fly ash ratio (0, 0.11, 0.25, 0.42, and 0.66) of AAB soil. In addition, PF-AAB soil achieves higher reliability indices for all CBR_{min} COV relative to CHF-AAB-soil mixture. This change may be attributed to the fact that

PF induces higher interfacial friction mobilization (rough surfaces) in soil compared to the CHF-soil matrix. The reliability index for both PF and CHF AAB soils against CBR failure (β_{CBR}) values shows the linear pattern of increase with an increase in fiber content and decrease with an increase in COV, and this pattern is in agreement with those of Moghal et al. (2017, 2018a). It is also interesting to emphasize in Fig. 12c that there is high variability in COV of CBR_{min} ($\geq$30%) for both $\beta_{CBR\text{-}PF}$ and $\beta_{CBR\text{-}CHF}$; the maximum reliability index reaches up to 3, which can be an acceptable performance of soil subgrade strength. Figure 12d represents that the reliability index's magnitude reduces due to higher COV of CBR_{min} = 40% under the same proportions of slag-fly ash and fibers.

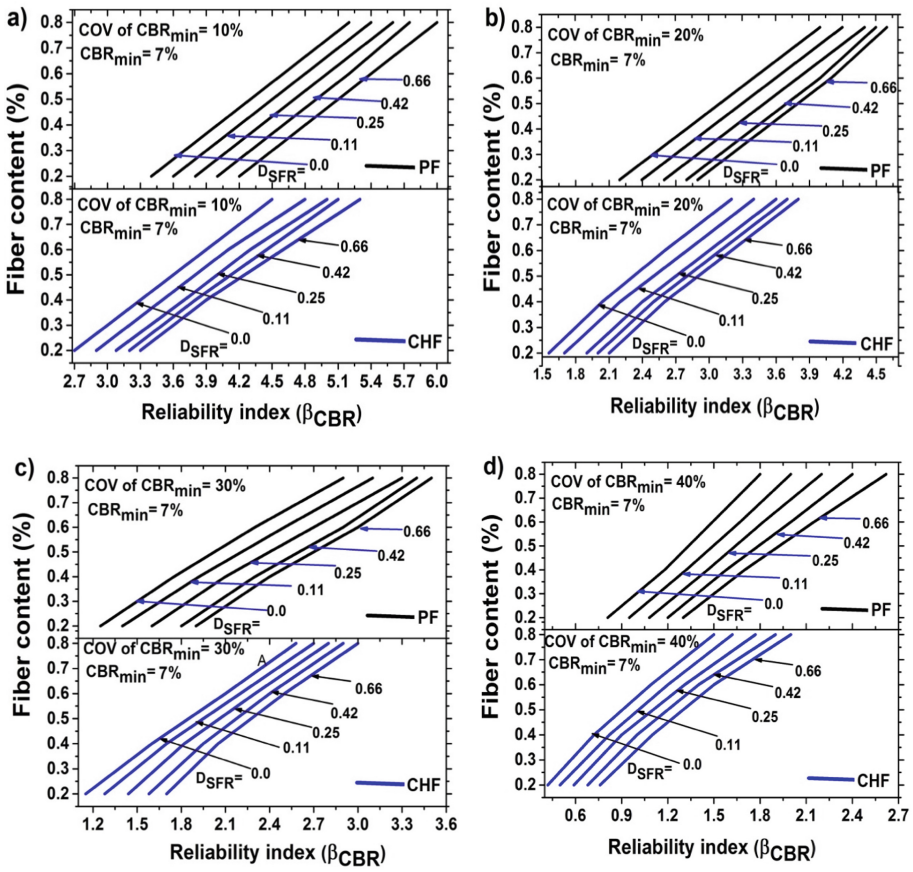

Fig. 12. Variation of reliability index against CBR failure (β_{CBR}) for both PF, CHF-AAB soils with varying slag-fly ash ratio at different COV a) 10%; b) 20%; c) 30%; d) 40%.

It may be noted that the use of high dosages of alkaline binders in the soil does not produce any volatile compounds. Besides, the heavy metals leaching from the mixture of fly ash and slag is very negligible. The heavy metals such as chromium (Cr), arsenic

trioxide (AS_2O_3), lead oxide (PbO), and zinc oxide (ZnO) are not present in fly ash and slag. The chemical compound of fly ash and slag (such as Cao, MgO) can easily monitor the pH and leachate, which does not impact the surrounding flora and fauna significantly. However, the manufacturing process of AAB manufacturing does not generate any CO_2 emissions as it utilizes already available industrial wastes as raw materials compared to Portland cement (PC), which emits almost to 750–850 kg CO_2e/ton for 1 ton of Portland cement production. Polypropylene and hemp fibers consume less natural resources to be produced. They are biodegradable and widely recyclable. Burning of PF and CHF does not generate toxic gases like chlorine. Hence a combination of AAB and CHF or PF is an eco-friendly solution.

5 Conclusions

The following conclusion are drawn from the geotechnical and microstructural studies:

- Substantial mobilization of friction and interfacial bonding made PF-soil offer higher penetration resistance than CHF-soil, regardless of the lime, cement, and slag/fly ash ratio in the AAB mixture.
- At 28 days of curing, geotechnical studies showed that the fiber-AAB-soil mixtures had achieved 32% and 58% higher compressive shear strength, 47%, and 79% higher subgrade strength bearing ratio (in terms of CBR strength) relative to fiber-cemented and lime-fiber reinforced soils.
- With the increasing replacement of fly ash with slag content (0 to 40%) in the AAB mix, soil compressibility (in terms of void ratio and swelling potential) decreases. The volumetric stability of both AAB and cemented soil has been greatly improved through the development of active pozzolanic cementitious products.
- Microstructural studies have identified new molecular bonds and crystalline phases around the cemented lime and alkaline clay matrix. Moreover, the PF and CHF-AAB-soil micrographs formed the spatial thread bridge network surface, regulating the tensile cracks around the subgrade layers
- Elastic modulus and modulus of rupture of soil increase with fiber and slag content; this improvement is proportional to the increase in ITS and UCS values, which substantially regulate the flexural and tensile crack propagation.
- The reliability index for both $\beta_{CBR\text{-}PF}$ and $\beta_{CBR\text{-}CHF}$ AAB-soils against the subgrade strength failures decreases with an increase in COV of CBR_{min}. Based on the findings, it is recommended that adding up to 0.8% of fiber (both PF and CHF) and 40% slag in alkaline soil mixture help to improve the subgrade stability significantly to a large extent.

Acknowledgments. The authors would like to express their sincere gratitude to the Central Analytical Laboratory Facilities at BITS-Pilani, Hyderabad Campus, for providing the setup for the FTIR, SEM/EDS, and XRD analyses.

References

Al-Mukhtar, M., Khattab, S., Alcover, J.-F.: Microstructure and geotechnical properties of lime-treated expansive clayey soil. Eng. Geol. **139–140**, 17–27 (2012). https://doi.org/10.1016/j.enggeo.2012.04.004

Amadi, A.A.: Enhancing durability of quarry fines modified black cotton soil subgrade with cement kiln dust stabilization. Transp. Geotech. **1**(1), 55–61 (2014)

Anggraini, V., Asadi, A., Farzadnia, N., Jahangirian, H., Huat, B.B.K.: Reinforcement benefits of nanomodified coir fiber in lime-treated marine clay. J. Mater. Civ. Eng. **28**(6), 1–8 (2016)

Bell, F.G.: Lime stabilization of clay minerals and soils. Eng. Geol. **42**(4), 223–237 (1996)

Bordoloi, S., Garg, A., Sekharan, S.: A Review of physio-biochemical properties of natural fibers and their application in soil reinforcement. Adv. Civil Eng. Mater. **6**(1), 20160076 (2017)

Chandra, S., Viladkar, M.N., Nagrale, P.P.: Mechanistic approach for fiber-reinforced flexible pavements. J. Transp. Eng. **134**(1), 15–23 (2007)

Correia, A.A.S., Venda Oliveira, P.J., Custódio, D.G.: Effect of polypropylene fibres on the compressive and tensile strength of a soft soil, artificially stabilised with binders. Geotext. Geomembr. **43**(2), 97–106 (2015)

Cristelo, N., Cunha, V.M.C.F., Dias, M., Gomes, A.T., Miranda, T., Araújo, N.: Influence of discrete fibre reinforcement on the uniaxial compression response and seismic wave velocity of a cement-stabilised sandy-clay. Geotext. Geomembr. **43**(1), 1–13 (2015)

Davidovits, J.: Properties of geopolymer cements. Alkaline Cements and Concretes, Kiev, Ukraine, pp. 1–19 (1994)

Elkhebu, A., et al.: Effect of incorporating multifilament polypropylene fibers into alkaline activated fly ash soil mixtures. Soils Found. Jpa. Geotech. Soc. **59**(6), 2144–2154 (2020)

GuhaRay, A., Baidya, D.K.: Reliability-based analysis of cantilever sheet pile walls backfilled with different soil types using the finite-element approach. Int. J. Geomech. **15**(6), 1–11 (2015)

Jiang, N.J., Du, Y.J., Liu, K.: Durability of lightweight alkali-activated ground granulated blast furnace slag (GGBS) stabilized clayey soils subjected to sulfate attack. Appl. Clay Sci. **161**(April), 70–75 (2018)

Kutanaei, S.S., Choobbasti, A.J.: Effects of nanosilica particles and randomly distributed fibers on the ultrasonic pulse velocity and mechanical properties of cemented sand. J. Mater. Civ. Eng. **29**(3), 1–9 (2017)

Mazhoud, B., Collet, F., Pretot, S., Lanos, C.: Mechanical properties of hemp-clay and hemp stabilized clay composites. Constr. Build. Mater. **155**, 1126–1137 (2017)

Miao, S., et al.: Mineral abundances quantification to reveal the swelling property of the black cotton soil in Kenya. Appl. Clay Sci. **161**, 524–532 (2018). https://doi.org/10.1016/j.clay.2018.02.003

Miao, S., Wei, C., Huang, X., Shen, Z., Wang, X., Luo, F.: Stabilization of highly expansive black cotton soils by means of geopolymerization. J. Mater. Civ. Eng. **29**(10), 04017170 (2017)

Moghal, A.A.B., Chittoori, B.C.S., Basha, B.M.: Effect of fibre reinforcement on CBR behaviour of lime-blended expansive soils: reliability approach. Road Mater. Pav. Des. **19**(3), 690–709 (2018a)

Moghal, A.A.B., Chittoori, B.C.S., Basha, B.M., Al-Mahbashi, A.M.: Effect of polypropylene fibre reinforcement on the consolidation, swell and shrinkage behaviour of lime-blended expansive soil. Int. J. Geotech. Eng. **12**(5), 462–471 (2018b)

Moghal, A.A.B., Chittoori, B.C.S., Basha, B.M., Al-Shamrani, M.A.: Target reliability approach to study the effect of fiber reinforcement on UCS behavior of lime treated semiarid soil. J. Mater. Civ. Eng. **29**(6), 04017014 (2017)

Murmu, A.L., Dhole, N., Patel, A.: Stabilisation of black cotton soil for subgrade application using fly ash geopolymer. Road Mater. Pav. Des. 0(0), 1–19 (2018)

Pourakbar.: Application of alkali-activated agro-waste reinforced with wollastonite fibers in soil stabilization. J. Mater. Civ. Eng. **29**(2), 04016206 (2016)

Pourakbar, S., Huat, B.B.K.: Laboratory-scale model of reinforced alkali-activated agro-waste for clayey soil stabilization. Adv. Civil Eng. Mater. **6**(1), 20160023 (2017)

Provis, J.L., Deventer, J.S.J. (eds.): Alkali activated materials. RSR, vol. 13. Springer, Dordrecht (2014). https://doi.org/10.1007/978-94-007-7672-2

Rios, S., Cristelo, N., Viana, A., da Fonseca, C.F.: Structural performance of alkali-activated soil ash versus soil cement. J. Mater. Civil Eng. **28**(2), 04015125 (2016). https://doi.org/10.1061/(ASCE)MT.1943-5533.0001398

Saride, S., Dutta, T.: Effect of fly-ash stabilization on stiffness modulus degradation of expansive clays. J. Mater. Civil Eng. **28**(12), 04016166 (2016). https://doi.org/10.1061/(ASCE)MT.1943-5533.0001678

Sivapullaiah, P.V., Sankara, G., Allam, M.M.: Mineralogical changes and geotechnical properties of an expansive soil interacted with caustic solution. Environ. Earth Sci. **60**(6), 1189–1199 (2010)

Sudhakaran, S.P., Sharma, A.K., Kolathayar, S.: Soil stabilization using bottom ash and areca fiber: experimental investigations and reliability analysis. J. Mater. Civ. Eng. **30**(8), 1–10 (2018)

Syed, M., Guharay, A.: Effect of fiber reinforcement on mechanical behavior of alkali-activated binder-treated expansive soil: reliability-based approach. Int. J. Geomech. ASCE **20**(12), 1–14 (2020)

Syed, M., GuhaRay, A., Goel, D., Asati, K., Peng, L.: Effect of freeze–thaw cycles on black cotton soil reinforced with coir and hemp fibres in alkali-activated binder. Int. J. Geosynt. Ground Eng. **6**(2),(2020a). https://doi.org/10.1007/s40891-020-00200-7

Syed, M., GuhaRay, A., Kar, A.: Stabilization of expansive clayey soil with alkali activated binders. Geotech. Geol. Eng. **38**(6), 6657–6677 (2020b). https://doi.org/10.1007/s10706-020-01461-9

Tang, C.-S., Shi, B., Li, J., Wang, D.-Y., Cui, Y.-J.: Tensile strength of fiber-reinforced soil. J. Mater. Civ. Eng. **28**(7), 04016031 (2016)

Tang, C., Shi, B., Gao, W., Chen, F., Cai, Y.: Strength and mechanical behavior of short polypropylene fiber reinforced and cement stabilized clayey soil. Geotext. Geomembr. **25**(3), 194–202 (2007)

Wei, L., Chai, S., Zhang, H., Shi, Q.: Mechanical properties of soil reinforced with both lime and four kinds of fiber. Constr. Build. Mater. **172**, 300–308 (2018). https://doi.org/10.1016/j.conbuildmat.2018.03.248

Yetimoglu, T., Inanir, M., Inanir, O.E.: A study on bearing capacity of randomly distributed fiber-reinforced sand fills overlying soft clay. Geotext. Geomembr. **23**(2), 174–183 (2005)

Yong, R.N., Ouhadi, V.R.: Experimental study on instability of bases on natural and lime/cement-stabilized clayey soils. Appl. Clay Sci. **35**(3–4), 238–249 (2007)

Zevgolis, I.E., Bourdeau, P.L.: Probabilistic analysis of retaining walls _ Elsevier Enhanced Reader.pdf. Comput. Geotech. (2010)

Zhang, M., Guo, H., El-Korchi, T., Zhang, G., Tao, M.: Experimental feasibility study of geopolymer as the next-generation soil stabilizer. Constr. Build. Mater. **47**, 1468–1478 (2013)